

The Airborne Cloud-Aerosol Transport System (ACATS) is a lidar system that is both a Doppler lidar and a high spectral resolution lidar (HSRL). ACATS has advanced component technologies and produced an airborne instrument directly applicable to prototyping and validation for future space-based lidars. Demonstration flights of the ACATS instrument are funded by the Airborne Instrument Technology Transition (AITT) program.

- ACATS test flights on the NASA ER-2 aircraft occurred in Feb. 2012.
- The HSRL aspect of ACATS separates the particulate and molecular components (unlike standard backscatter lidar which only measure total backscatter) and allows for direct retrievals of extinction.
- The Doppler aspect adds capability to derive wind motion.
- A high-resolution interferometer is used to provide the spectral discrimination needed for the Doppler shift and HSRL measurement.

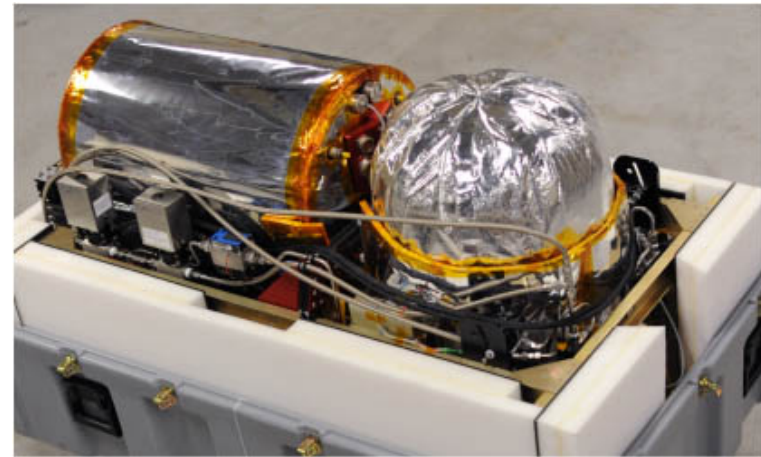


Figure 1. A photo of the ACATS instrument as currently configured. The insulated tube on the left side contains the receiver subsystem, including a Fabry-Perot interferometer. The insulated dome on the right side houses the telescope.

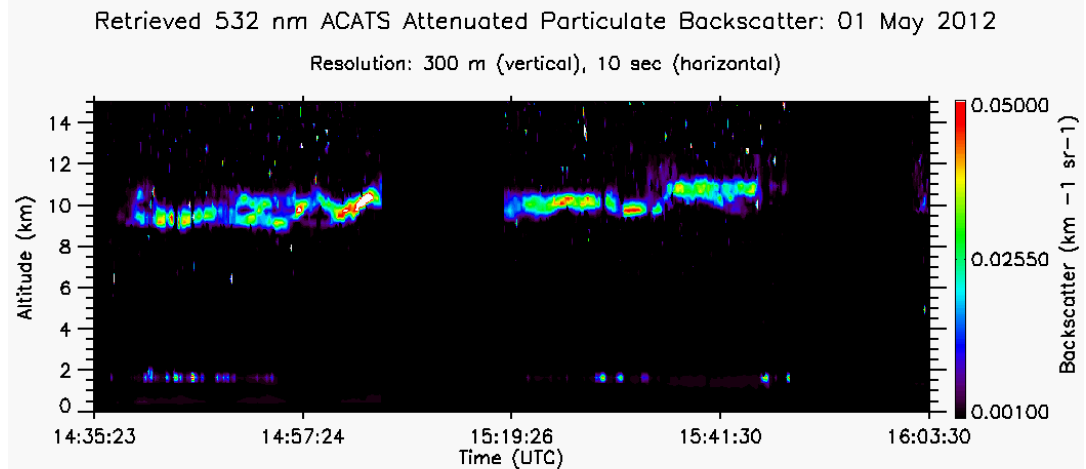


Figure 2. An example of the retrieved ACATS particulate backscatter ($\text{km}^{-1}\text{sr}^{-1}$) from 1 May 2012 shows cirrus clouds at an altitude of about 10 km and demonstrates the HSRL nature of the direct particulate backscatter measurement.



Name: John E. Yorks, NASA/GSFC, Code 612 and SSAI
E-mail: John.E.Yorks@nasa.gov
Phone: 301-614-6284



Yorks, J. E., M. McGill, V.S. Scott, D. Hlavka and W. Hart, A High Altitude Cloud-Aerosol Transport Lidar System, *Proceedings of the 25th International Laser-Radar Conference*, Saint Petersburg, Russia, July 5-10, 2010.

McGill, M.J., W.R. Skinner, and T.D. Irgang, "Analysis techniques for the recovery of winds and backscatter coefficients from a multiple channel incoherent Doppler lidar," *Applied Optics*, 36, 1253-1268, 1997a.

Data Sources: The Airborne Cloud-Aerosol Transport System (ACATS) data products are still currently under development. Here, the backscatter data is averaged to a 2 km horizontal resolution and 300 m vertical resolution. The ACATS data was collected during test flights in Feb. 2012 and during ground testing at NASA Goddard Space Flight Center in April/May 2012.

Technical Description of Figures:

Figure 1. A photo of the ACATS instrument as currently configured. The insulated dome on the right side houses the 8 inch telescope, which collects the backscattered light at a 45 degree view angle and passes it through to the receiver subsystem (the insulated tube on the left side). The primary difference between a lidar system capable of only measuring total signal intensity (e.g., CALIPSO) and an instrument that directly measures particulate extinction and Doppler shifts (e.g. ACATS) lies in the receiver subsystem. The focus of the ACATS receiver system is an optical filter known as a Fabry-Perot interferometer (also termed etalon). The etalon provides the spectral resolution needed to resolve the HSRL measurement and the Doppler shift inherent in the backscattered signal. The ACATS laser (not visible in Figure 1) is an injection-seeded Nd:YAG laser with output of 10 mJ per pulse at 532 nm.

Figure 2. An example of the retrieved ACATS particulate backscatter ($\text{km}^{-1}\text{sr}^{-1}$) from ground testing on 1 May 2012 shows cirrus clouds at an altitude of about 10 km and boundary layer cumulus clouds at 1.5 km. The two data gaps, before 15:19:26 and 16:03:30 UTC, are time periods when the etalon calibration occurs. The data is averaged to 300 m vertically and 10 seconds to reduce noise in the signal. The ACATS lidar fundamentally measures the particulate backscatter (bottom), Rayleigh backscatter, and Doppler Shift as a function of altitude at 532 nm wavelength. Wind speed and direction is determined from the Doppler shift, while the separation of the particulate and Rayleigh backscatter allows the ACATS instruments to directly retrieve profiles of extinction.

Scientific significance: Cloud and aerosol properties have a significant influence on the earth's climate system. Obtaining an accurate assessment of cloud and aerosol properties and their influences on the atmospheric radiation budget remain a major challenge in understanding and predicting the climate system. The ACATS data products have a large range of applications to significant climate system issues, such as examining cirrus optical properties and convective outflow in cirrus anvils, assessing dust and smoke transport, and investigating cloud-aerosol interactions and radiative effects.

Relevance for future science and relationship to Decadal Survey: ACATS should contribute to future space-based missions by advancing component technologies and by producing an airborne instrument directly applicable to prototyping and validation for NASA's Cloud-Aerosol Transport System (CATS), Aerosol-Cloud-Ecosystem (ACE) and 3-D Winds missions. For example, the current algorithm development for ACATS data products will be used for algorithm development of the International Space Stations (ISS) CATS instrument.



Simulating Extreme Rainfall using the NASA Unified Weather Research and Forecasting Model

Wei-Kuo Tao, Roger Shi*, Stephen Lang†, Code 612, NASA/GSFC, *GESTAR/MSU, †SSAI

Typhoon Morakot hit Taiwan on the night of 7 August 2009 as a Category 1 storm and caused up to 3000 mm of rain, leading to the worst flooding there in 50 years, as well as devastating mudslides, which resulted in nearly 700 casualties. The 3000-mm rainfall has been ranked by the WMO as the 2nd highest rainfall total by a single storm. We conducted simulations of Morakot with the NASA Unified Weather Research and Forecasting model (NU-WRF) at high resolution (2-km inner grid spacing) to understand the development of this extreme weather event.

- NU-WRF, using the Goddard microphysics and radiation schemes, was able to capture the amount and location of the observed surface rainfall.
- The simulations showed that the typhoon-induced circulation, orographic lifting, and a moisture-abundant southwest monsoon flow were responsible for the tremendous rainfall in this case.
- The high correlation between simulated and observed rainfall was due to good agreement between the simulated and observed storm tracks and intensities.

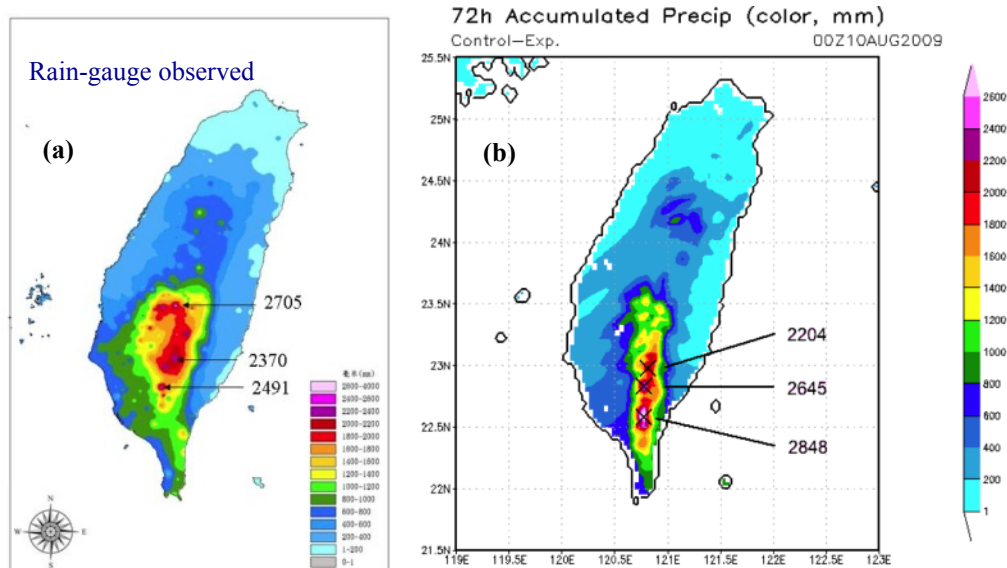


Figure 1. (a) Rain-gauge observed and (b) model-accumulated rainfall from 0000 UTC August 7 to 0000 UTC August 10 2009.

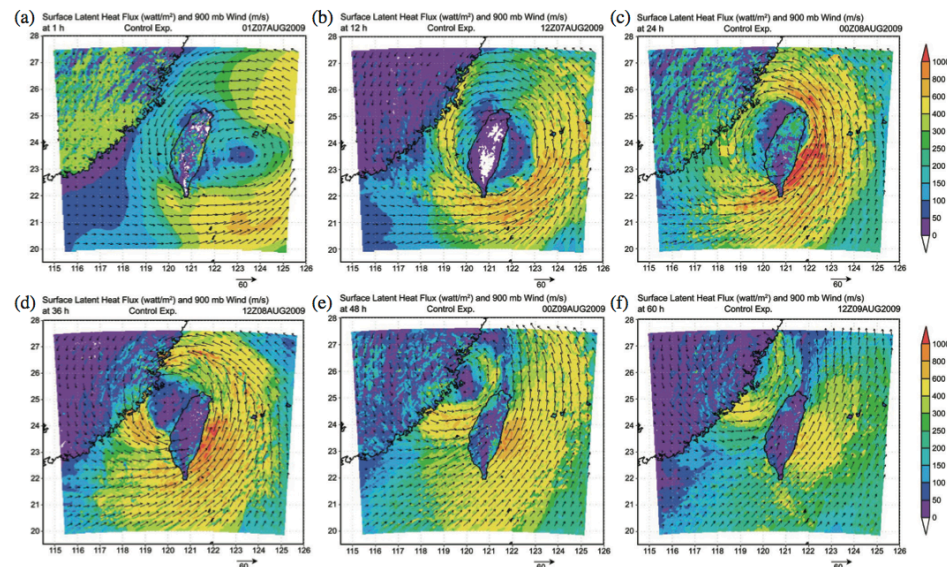


Figure 2. Simulated surface latent heat flux (W m^{-2} , shaded) and 900 hPa wind (m s^{-1} , vectors) at (a) 1, (b) 12, (c) 24, (d) 36, (e) 48 and (f) 60 hours of integration from the NU-WRF run.



Name: Wei-Kuo Tao, NASA/GSFC, Code 612
E-mail: wei-kuo.tao-1@nasa.gov
Phone: 301-614-6269

References:

Tao, W.-K., J. J. Shi, P.-L. Lin, J. Chen, S. Lang, M.-Y. Chang, M.-J. Yang, C.-C. Wu, C. Peters-Lidard, C.-H. Sui, and B. J.-D. Jou, 2011: High-resolution numerical simulation of the extreme rainfall associated with Typhoon Morakot. Part I: Comparing the impact of microphysics and PBL parameterizations with observations. *Terrestrial, Atmospheric, and Ocean Sciences*, **22**, 673-696.

Lang, S. E., W. K. Tao, X. Zeng, and Y. Li, 2011: Reducing the biases in simulated radar reflectivities from a bulk microphysics scheme: Tropical convective systems. *Journal of the Atmospheric Sciences*, **68**, 2306-2320.

Data Sources: Accumulated surface rainfall data from more than 600 rain gauge stations and surface radar reflectivity data from radar stations in Taiwan.

Technical Description of Figures:

Figure 1. (a) Rain-gauge observed and (b) model-accumulated rainfall from 0000 UTC August 7 to 0000 UTC August 10 2009. The numbers in the figure indicate the location and total rainfall amount. The model rainfall accumulations shown in (b) are based on the simulated rainfall in the inner domain (2-km grid spacing). The observed rainfall accumulations are based on the estimates from surface rain gauge stations in Taiwan. The good agreement in these features between the model and observations can be attributed to good agreement between the simulated and observed storm tracks and intensities.

Figure 2. Simulated surface latent heat flux (W m^{-2} , shaded) and 900 hPa wind (m s^{-1} , vectors) at (a) 1, (b) 12, (c) 24, (d) 36, (e) 48 and (f) 60 hours of integration from the NU-WRF run. Greatly enhanced latent heat flux and Taiwan's unique terrain were the main factors that determined the location of the heavy precipitation. The typhoon-circulation reinforced the large-scale southwesterly circulation over the warm Taiwan Strait, accelerating the ocean-surface latent heat flux. Convective systems generated over the Taiwan Strait were then intensified by orographic lifting due to Taiwan's steep mountain terrain as they propagated inland.

Scientific significance:

The results indicate that the high-resolution NU-WRF is capable of simulating the tremendous rainfall (the maximum rainfall exceeds 2800 mm over a 72-h integration) observed in this case as well as the elongated rainfall pattern in the southwest-northeast direction and the heavily concentrated north-south line over southern Taiwan that was also observed. The improved Goddard microphysics scheme reduced the amount of graupel and increased the amount of snow and cloud ice as with the cases shown in Lang et al. (2011). The stronger storm simulated with the improved physics is a result of less evaporative cooling from cloud droplets and consequently weaker simulated downdrafts.

Relevance for future science and relationship to Decadal Survey:

This work improves our understanding of how tropical cyclones interact with the larger-scale circulation and coastal terrain to produce extreme rainfall and landslide events. This work can provide context for the analysis of data from 2012-2014 Hurricane and Severe Storm Sentinel (HS3) Earth Venture-1 campaign and for future research on extreme rainfall events using future data products from the Global Precipitation Mission (GPM) set to launch in 2014.



Hailstorm, Tornado, and Rainfall in 2011 Consistent with Weekly Cycles Observed in Earlier Years

Thomas L. Bell, Emeritus Code 613, NASA GSFC

Two recent papers (by Rosenfeld and Bell 2011; and Bell et al. 2008) contained figures showing the day of the week favored by hailstorms, tornadoes, and rainfall for each summer for 1995–2009 in the case of hailstorms and tornadoes and for 1998–2006 for rainfall estimated with a multi-satellite system including TRMM (Tropical Rainfall Measuring Mission). There is a clear tendency for storms to avoid weekends — particularly for hailstorms and rainfall, possibly because there are many more hailstorms and rain events than tornadoes and the statistics for hailstorms and rainfall are clearer as a consequence. Data through 2011 are now available, and updated figures are shown here. The weekly cycles detected for the past few years are rather weak (“balloons” near the origin) but are consistent with the patterns seen in earlier years.

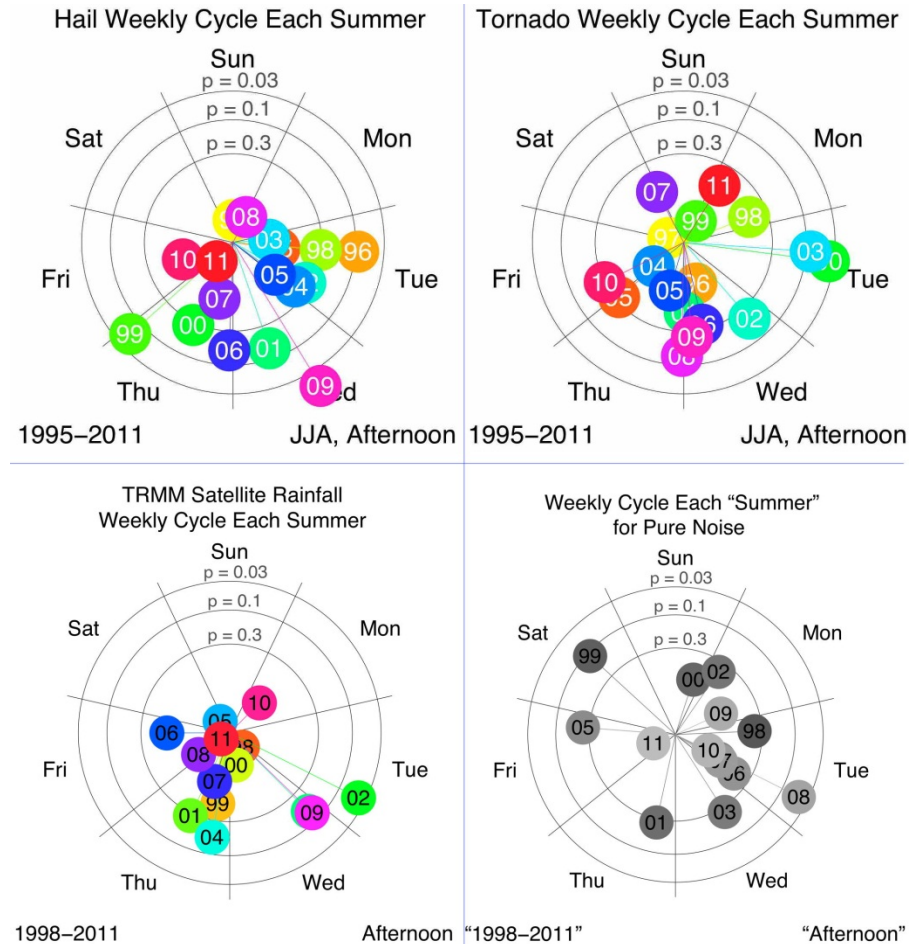


Figure 1: The clock plots above indicate the day of the week during the summer months when maximum atmospheric activity is observed for three kinds of data: hailstorms, tornadoes, and rainfall. There is a colored balloon for each year, inscribed with the year represented. The further from the origin a balloon is, the stronger the weekly cycle was in the data. The gray image (bottom right) shows what a clock plot might look like if no weekly cycle was actually present in the data.



References:

1. Rosenfeld, D., and T. L. Bell (2011): Why do tornados and hailstorms rest on weekends? *Journal of Geophysical Research*, **116**, D20211, doi: 10.1029/2011JD016214.
2. Bell, T. L., D. Rosenfeld, K.-M. Kim, J.-M. Yoo, M.-I. Lee, and M. Hahnenberger (2008), Midweek increase in U.S. summer rain and storm heights suggests air pollution invigorates rainstorms, *Journal of Geophysical Research*, **113**, D02209, doi:10.1029/2007JD008623.

Data Sources: Data for hailstorms and tornadoes are provided by NOAA's Storm Prediction Center [SPC], in the form of lists of locations, times, and strengths of hailstorms or tornadoes, available from the web site <http://www.spc.noaa.gov/wcm/index.html#data>. Data for rainfall are derived from TMPA data provided by the Giovanni web site: http://gdata1.sci.gsfc.nasa.gov/daac-bin/G3/gui.cgi?instance_id=TRMM_3-Hourly.

Technical Description of Figures:

Figure 1: Summertime occurrences of storms over the U.S. east of longitude 100W were counted for each day of a given summer (Jun-Aug, 92 days). The mean rate of occurrence for each day of the week was fit to a 7-day sinusoidal curve, and a “balloon” is placed on the clock plot in the sector corresponding to the day when the sinusoidal fit peaks. The statistical significance of the fit is estimated from the quality of the fit, and a “signal-to-noise” ratio for the fit is used to determine the radial location of the balloon. The “*p*-values” labeling the circles indicate the probabilities that data consisting of pure noise (unpredictable weather variations) could accidentally produce sinusoids with signal-to-noise values outside the given circle. Note that a single summer of data, 13 weeks, has only 13 “samples” -- statistics derived from so few samples are correspondingly noisy. There are about 7 times as many recorded hailstorms as tornados, and the clock plot for hailstorms presents us with a clearer statistical picture than the one for tornadoes. Rainfall data are averaged over the “non-coastal southeast” U.S., defined as longitudes 100W–80W and latitudes 32.5N–40N. The limitation in latitude is dictated by the coverage of the TRMM satellite.

Although the distribution of balloons (avoidance of weekends), is very suggestive, a better test of the statistical significance of the weekly cycles in the data is obtained by analyzing all summers of data together. If this is done, the weekly cycles of hailstorms and rainfall are highly significant (*p*-values 0.001 and 0.005 respectively), while the weekly cycle of tornadoes tests out with a *p*-value of 0.06.

Scientific significance: This study reinforces and extends the conclusions reached in earlier studies using TRMM data that showed that both rainfall area and rain intensity increase in the middle of the week over the SE U.S. during the summertime. The changes, when averaged over 15 years of data, are highly significant statistically. If the theory behind the changes seen in the averages are correct, human pollution can change weather in profound ways that are entirely distinct from “greenhouse warming”. Human pollution can shift rain patterns and cause increases in tornado and hailstorm frequency in areas susceptible to the influence of aerosols (identified in the theory as areas both with high humidity and unstable to the formation of intense storms, and where cloud bases are well below the freezing level of the atmosphere, as occurs over the eastern U.S. during the summer). Humans are, in effect, changing the climate back and forth every week, by shifting aerosol pollution levels above and below the background average each week. This causes one to ask, “How has the background level of aerosols itself changed the weather we experience?”

Current weather forecast models do not include the effects of changing aerosol pollution, partly because it is not well observed. Weather forecasts are therefore not yet capable of warning us of changes in storm intensities caused by different pollution levels.

Relevance for future science and relationship to Decadal Survey: This research is highly relevant to several of the challenges contained in the Decadal Survey: for climate changes as reflected in changes in severe storm behavior and rainfall patterns, and for weather forecasting. It underlines the need for monitoring aerosol concentrations in the atmosphere on a continuing basis.



An Unexpected Atmospheric Response to the 11-Year Solar Cycle

APL

William H. Swartz, NASA/GSFC/Code 614 and JHU/APL

R. S. Stolarski, JHU; L. D. Oman, E. L. Fleming, and C. H. Jackman, NASA/GSFC

The Sun's radiation (flux) output varies over an 11-year cycle. Our study looks at how the atmosphere responds to the 11-year solar cycle with two state-of-the-art chemistry–climate models (CCMs): the 3-D GEOSCCM and the GSFC 2-D coupled model. We compare and contrast how the model atmosphere responds to both the long-accepted solar cycle typically used in climate projections, developed at the Naval Research Laboratory (NRL), and the solar cycle inferred from NASA's SORCE satellite mission.

Our study explains why GCMs without coupled chemistry underestimate the temperature response to the solar cycle. Further, we show how different wavelength regions of the solar spectrum contribute to the middle atmosphere ozone response (see Fig. 2), and how the solar cycle signals derived from the SORCE instruments measuring these different regions lead to surprising model outcomes (see Fig. 1).

Although the solar forcing of climate is presently thought to be an order of magnitude smaller than anthropogenic factors, our scientific understanding of the solar influence is low. This study provides a path forward for a more general understanding and prediction of the atmosphere/climate response to solar variations.

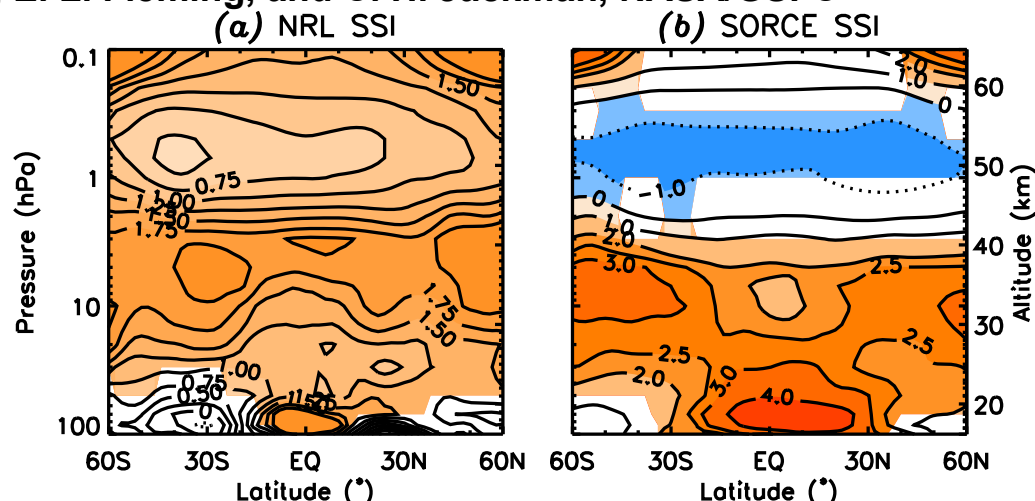


Figure 1: Simulated response of ozone to the solar cycle (O_3 change (%)) for solar maximum vs. minimum conditions in the GEOSCCM using the (a) NRL and (b) SORCE solar flux. The colored (non-white) portions of the plots indicate regions where the ozone response is statistically significant. At the top of the stratosphere near 50 km, the SORCE solar flux produces net ozone loss in the model (blue shaded region), which is unexpected.

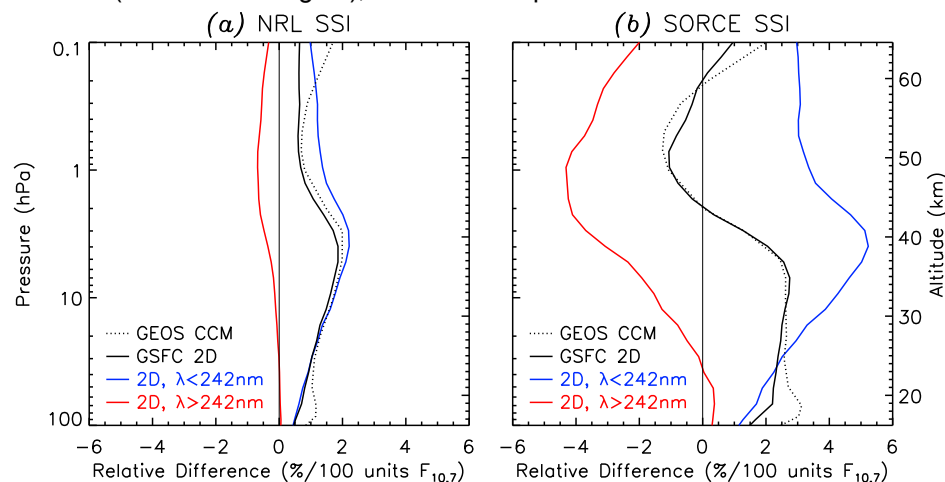


Figure 2: Simulated response of ozone to the solar cycle in the GSFC 2-D model in different wavelength ranges. The model shows how the solar cycle at wavelengths shorter than 242 nm lead to net production of ozone (in blue), while longer wavelengths lead to ozone loss (in red).



Name: William H. Swartz, NASA/GSFC/Code 614 and JHU/Applied Physics Laboratory
E-mail: bill.swartz@jhuapl.edu and swartz@polska.gsfc.nasa.gov
Phone: 240-228-8462

APL

References:

Swartz, W. H., R. S. Stolarski, L. D. Oman, E. L. Fleming, and C. H. Jackman (2012), Middle atmosphere response to different descriptions of the 11-yr solar cycle in spectral irradiance in a chemistry–climate model, *Atmospheric Chemistry and Physics Discussions*, 12, 7039–7071, doi:10.5194/acpd-12-7039-2012.

Data Sources: Solar flux data from the SORCE and UARS missions; total ozone data from TOMS, SBUV, and ground-based instruments; ozone profiles from SBUV, UARS/HALOE, and SAGE; microwave temperature profiles from SSU and MSU; solar radio flux data from NOAA; modeling simulations using the GEOSCCM and GSFC 2-D were performed at the NASA/Ames Advanced Supercomputing Division and at GSFC.

Technical Description of Figures:

Figure 1: Simulated response of ozone to the solar cycle (O_3 change (%) for solar maximum vs. minimum conditions) in the GEOSCCM using the (a) NRL and (b) SORCE solar flux. The colored (non-white) portions of the plots indicate regions where the ozone response is statistically significant (95% confidence level). The ozone response to the NRL solar flux is positive at all altitudes, up through the middle mesosphere. The response using the SORCE solar flux is very different in comparison. Although the ozone response in most of the stratosphere going from solar min to solar max is positive, or in phase with the solar cycle in total solar irradiance, above about 2 hPa the response is actually negative (up to 0.2 hPa), which is unexpected in view of the traditional understanding of solar variability.

Figure 2: Simulated response of ozone to the solar cycle in the GSFC 2-D model in different wavelength ranges. The model shows how the solar cycle at wavelengths shorter than 242 nm lead to net production of ozone, while longer wavelengths lead to ozone loss. The ozone responses at wavelengths less and greater than 242 nm are qualitatively similar for both the NRL and SORCE solar flux. The quantitative difference in the total responses between the two solar flux specifications results from the balance of the two wavelength regimes. The magnitude of the solar cycle in the short-wavelength part of the solar spectrum is greater for SORCE than the NRL solar flux, leading to a peak ozone production more than a factor of 2 larger. In the long-wavelength region, however, SORCE is greater by roughly a factor of 6 at its peak. The balance of these ozone production and loss regimes results in the very different total responses in the model when forced with the NRL and SORCE solar flux.

Scientific significance: This study provides a path forward for a more general understanding and prediction of the atmosphere/climate response to solar variations. The following are several significant science conclusions:

- Significantly different responses of the middle atmosphere are predicted for SORCE-derived solar flux changes in the ultraviolet compared to traditional (NRL)-derived solar cycle variability.
- Coupled chemistry is required to accurately model the temperature response (a typical GCM is not enough).
- Anti-phase ozone response (with respect to total solar irradiance) is explained by the mostly linear combination of the solar cycle in difference solar flux wavelength regions.

Relevance for future science and relationship to Decadal Survey: Although the solar forcing of climate is presently thought to be an order of magnitude smaller than anthropogenic factors, our scientific understanding of the solar influence is low. This work improves such understanding. The Decadal Survey has identified a continuous satellite record of solar irradiance as a priority. As such, this work is directly related to the ongoing SORCE mission as well as NASA's planned TSI Calibration Transfer Experiment (TCTE) and the Total and Spectral Solar Irradiance Sensor (TSIS) instruments on JPSS.